Investigation of the inorganic fluorides of different complexity

O. Matselko, J. Mlynáriková, Z. Vasková, B. Kubíková, Z. Netriová, M. Boča

Institute of Inorganic Chemistry, Slovak Academy of Sciences
Dúbravská cesta 9, Bratislava, 84536, Slovakia

Introduction. Fluorides are well known for their diverse industrial applications – *e.g.*, in extractive metallurgy, electrochemical processes, energy storage and transfer in solar power towers, as models for the electrochemical separation of lanthanides and actinides. In addition, intensive research projects concentrate on the optical properties of fluorides and use of the molten salt systems in the nuclear fuel industry – development of the Generation IV molten salt reactors.

Experimental. Phase identification, lattice parameters determination and crystal structure refinement were carried out using the room-temperature powder X-ray diffraction (XRD) data collected on Empyrean PANalytical diffractometer in Bragg-Brentano geometry (Cu *Kα* radiation; solid-state PIXcel detector). High temperature powder XRD experiments were performed using the Anton Paar heating attachment (HTK 16N High-Temperature Chamber with TCU 2000N Temperature Control Unit). Single crystal XRD data were collected at room temperature on Oxford diffraction CCD diffractometer Gemini (graphite monochromator, Mo *Kα* radiation) with an Atlas S2 CCD area detector. For the crystallographic calculations and structures visualization the following programs were used: WinCSD [1], Jana2006 [2], DIAMOND [3].Thermal properties of the studied compounds were investigated by means of the differential scanning calorimetry (DSC) performed with a NETZSCH Simultaneous Thermal Analyzer STA 449 F1 Jupiter. X-ray photoelectron spectroscopy (XPS) signals were recorded on the powdered samples using the NEXSA G2 XPS system (Thermo Fisher Scientific, UK) with a micro-focused monochromatic Al *Kα* X-ray source.

Results. For the systems $(LiF\text{-}CaF_2)_{eut}$-$n$$LnF_3$ (Ln = Nd, Sm, Gd; n = 0.01-0.4 (for Nd,Sm) / 0.3 (for Gd)) it has been found that, except crystallization of LiF, LnF_3 (Ln = Nd; n > 0.01), $Ln_{1-y}Ca_yF_{3-y}$ (Ln = Sm; n > 0.01) or $LiGdF_4$ (Ln = Gd; n ≥ 0.03), formation of cubic phases $\mathbf{Ca_{1-x}Ln_xF_{2+x}}$ (x ≈ 0.2-0.35 (Nd), 0.16-0.39 (Sm), 0.17-0.32 (Gd)) related to the fluorite-type structure is observed (space group *Fm*-3*m*). Starting values for the compositions of the cubic phases have been calculated according to the determined cell parameters and then refined with CeH_3 crystal structure model. Cell parameters of the cubic phases $Ca_{1-x}Ln_xF_{2+x}$ are changing with content of LnF_3 and, comparing three presented systems, are in agreement with an effect of lanthanide contraction. Pure CaF_2 is observed only in the samples with low content of LnF_3 (n ≤ 0.1).

Fluorides $\mathbf{A_3MF_7}$ – homocation K_3HfF_7, mixed cation Na_2KZrF_7 together with the new isostructural Na_2KHfF_7 and $Na_2K(Zr,Hf)F_7$ (refined composition $Na_2KZr_{0.53(1)}Hf_{0.47(1)}F_7$) – have been structurally characterized at room temperature by means of powder and single crystal XRD. Existence of the solid-solid phase transition at the elevated temperatures has been revealed during the differential scanning calorimetry experiments and further confirmed by the temperature dependent powder XRD. It has been found that K_3HfF_7 as well as K_3ZrF_7 undergoes to the reversible phase transition. Contrary, mixed cation compounds Na_2KZrF_7, Na_2KHfF_7 and $Na_2K(Zr_{0.5}Hf_{0.5})F_7$ are characterized by the irreversible transformations connected with the phase decomposition to homocation compounds over 400°C. XPS measurements confirmed the absence of oxygen in the crystal structures of studied compounds. It should be noted that Na_2KMF_7 (M = Zr, Hf or Zr/Hf) and K_3MF_7 (M = Zr, Hf) have similar thermal properties within the series. Nevertheless, the difference between Na_2KMF_7 and K_3MF_7 is significant. It can be concluded that Zr↔Hf replacement has low influence on properties, while Na↔K substitution effect is much stronger.

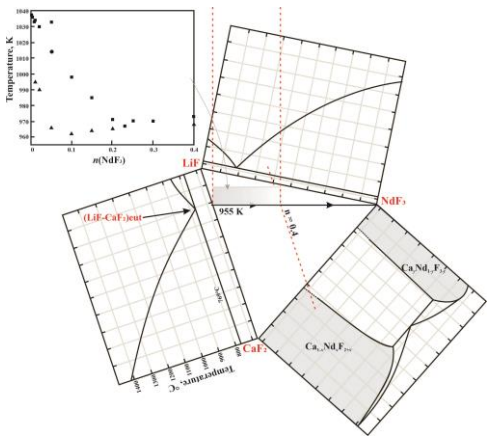

Figure 1. Partial quasi-binary phase diagram – $(LiF\text{-}CaF_2)_{eut}$-$n$$NdF_3$ [4], n ≤ 0.4 – together with the phase diagrams of the terminating binary systems

$Ca_{1-x}Ln_xF_{2+x}$ (Ln = Nd, Sm, Gd)

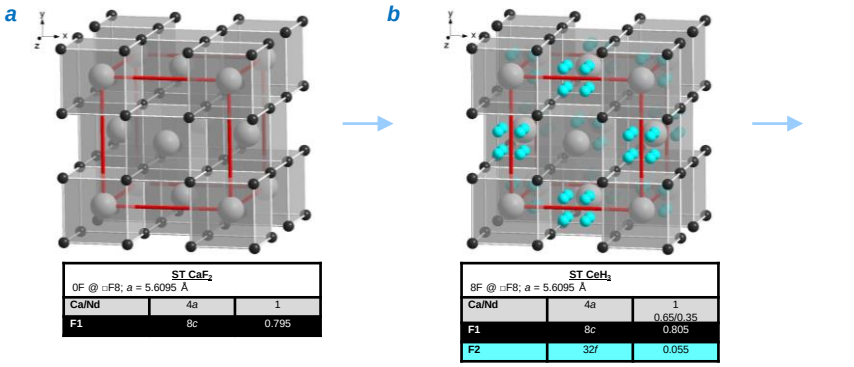

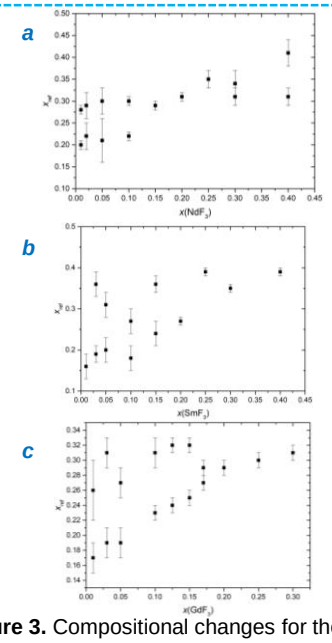

Figure 3. Compositional changes for the cubic phases $Ca_{1-x}Ln_xF_{2+x}$ within the concentration range for Ln = Nd (*a*), Sm (*b*), Gd (*c*)

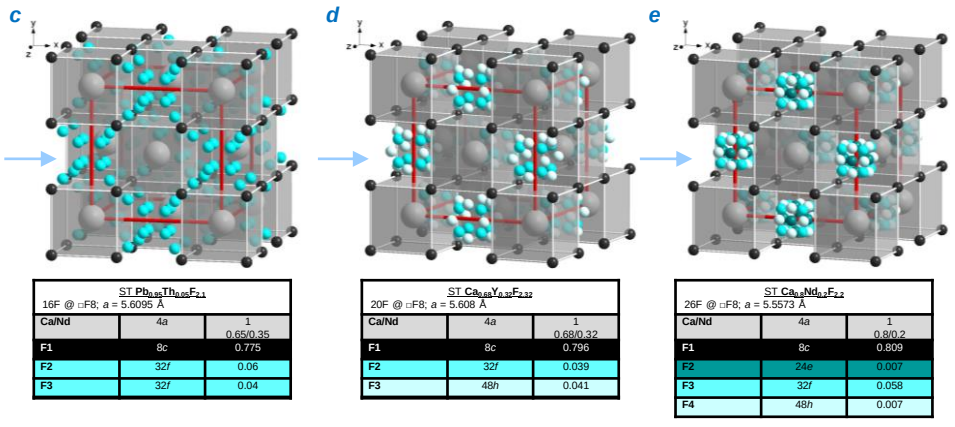

Figure 2. Crystal structures of $Ca_{1-x}Nd_xF_{2+x}$ [5] and crystallographic parameters (multiplicity of the atom position, site occupancy factor) for models in different structure types (space group *Fm*-3*m*): CaF_2 (*a*); CeH_3 (*b*); $Pb_{0.95}Th_{0.05}F_{2.1}$ (*c*); $Ca_{0.68}Y_{0.32}F_{2.32}$ (*d*); $Ca_{0.8}Nd_{0.2}F_{2.2}$ (*e*)

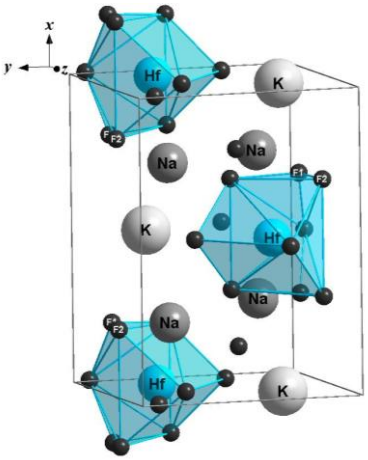

Figure 4. Unit cell of Na_2KHfF_7 along with coordination polyhedra of Hf atoms – $\{HfF_7\}$ units

Table 1. Experimental conditions and crystallographic parameters for Na_2KHfF_7

Compound composition		**Na_2KHfF_7**	
Formula weight		396.6	
Structure type		Na_2KZrF_7 [6]	
Pearson symbol		*oP*22	
Space group		*Pmn*2_1	
Unit-cell parameters:	*a* (Å)	8.213(2)	8.22624(8)*
	b (Å)	6.126(2)	6.13103(4)*
	c (Å)	5.979(2)	5.98505(6)*
Cell volume V (Å^3)		300.8(2)	301.858(5)*
Formula units per cell Z		2	
Density D_x (g·cm^{-3})		4.3783	
Radiation		Mo *K*α, λ = 0.71073 Å	
Absorption coefficient μ (mm^{-1})		18.247	
Number of reflections:	measured	4389	
	independent	806	
	with $I > 3\sigma(I)$	787	
Reliability factor R_{eq}		0.0331	
Range of *h*, *k*, *l*		$-10 \le h \le 10$, $-8 \le k \le 8$, $-7 \le l \le 7$	
θ_{max} (°)		30.01	
Reliability factors:	*R*	0.0232	
	wR	0.0654	
	S	1.2973	

*powder diffraction data

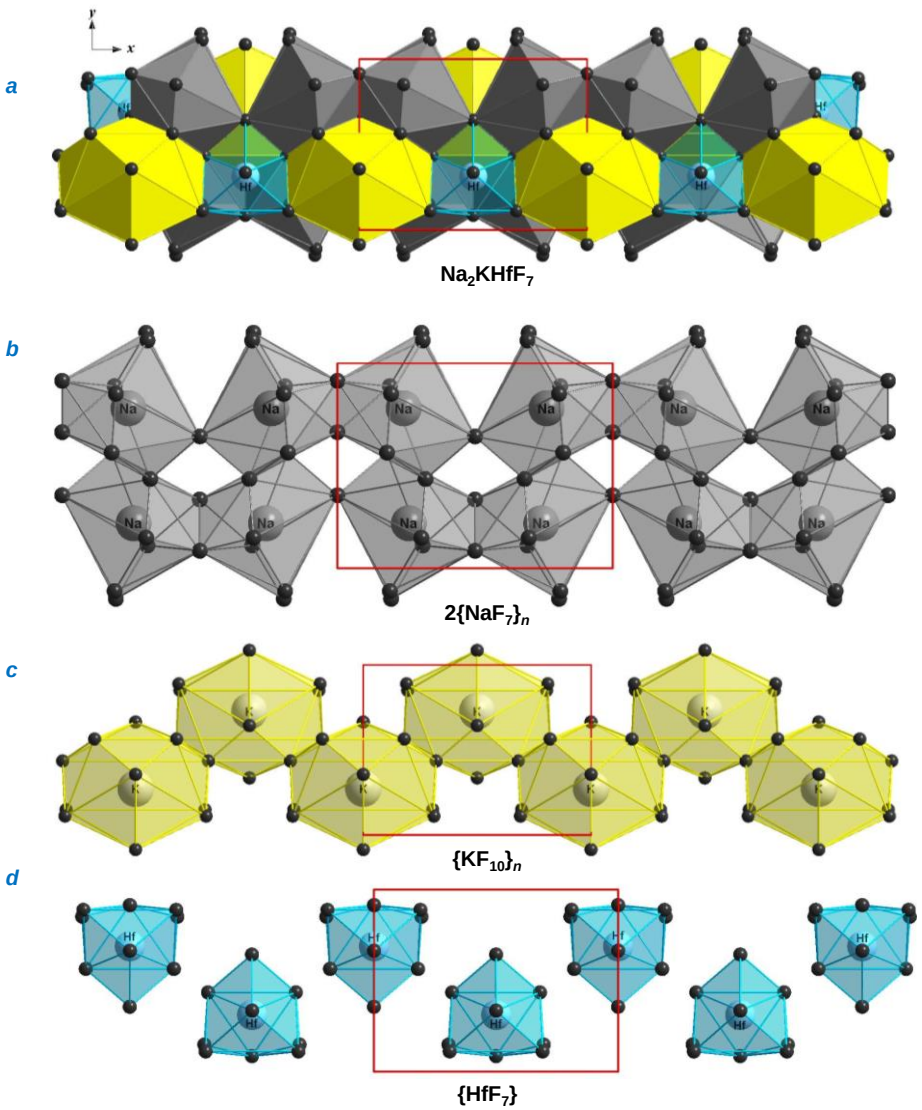

Figure 5. Crystal structure of Na_2KHfF_7 (*a*) as interpenetration of chains formed by coordination polyhedra around Na (*b*) and K (*c*) atoms and polyhedra around Hf (*d*) atoms; projection on *xy* plane

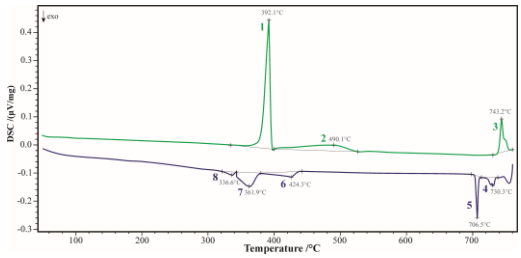

Figure 6. DSC records for Na_2KHfF_7

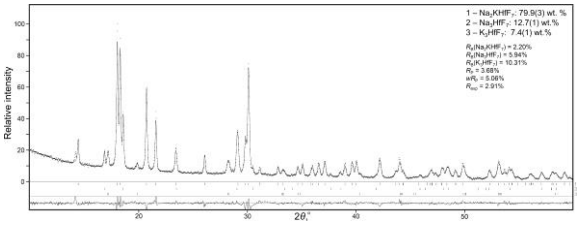

Figure 7. Phase composition of the samples Na_2KHfF_7 after the DSC measurements (heating till 760°C)

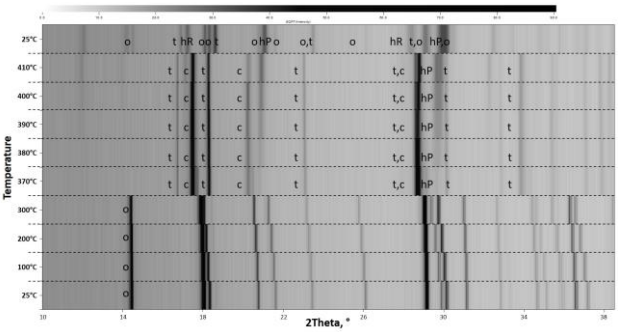

Figure 8. XRPD patterns (top view) for Na_2KHfF_7 representing phase transformations during heating till 410°C: o – Na_2KHfF_7 (space group $Pmn2_1$); t – Na_3HfF_7 (*I*4/*mmm*); c – K_3HfF_7 (*Fm*-3*m*); hP – $K_3Hf_{1.5}F_9$ (*P*-3*m*1)

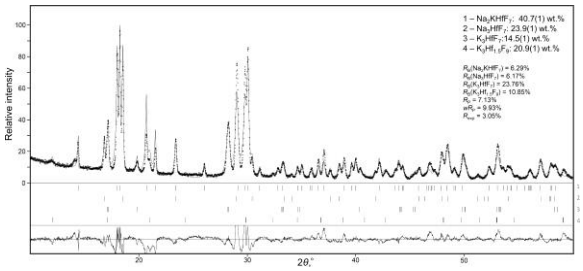

Figure 9. Phase composition of the samples Na_2KHfF_7 after the temperature dependent XRPD (heating till 410°C)

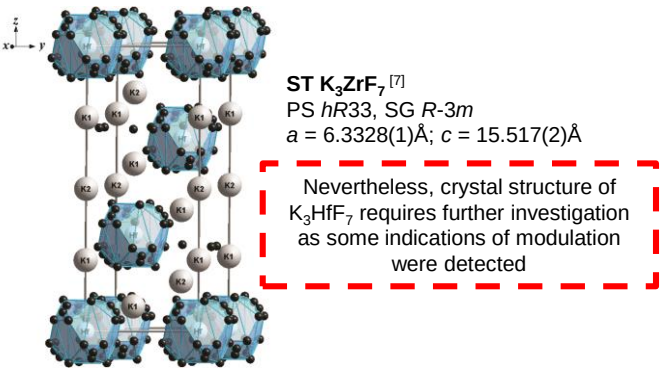

ST K_3ZrF_7 [7]
PS *hR*33, SG *R*-3*m*
a = 6.3328(1)Å; *c* = 15.517(2)Å

Nevertheless, crystal structure of K_3HfF_7 requires further investigation as some indications of modulation were detected

Figure 10. Unit cell of K_3HfF_7 and coordination polyhedra for Hf atoms – {HfF_7} units (considering SOF of F atoms)

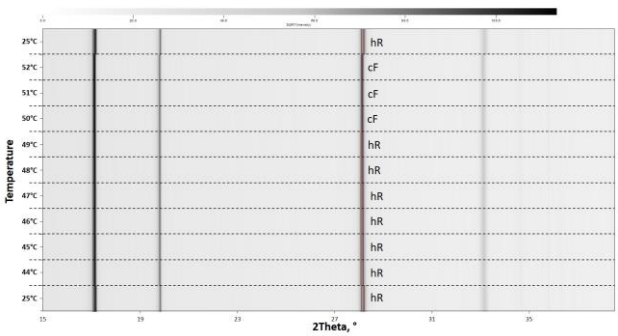

Figure 11. XRPD patterns (top view) for K_3HfF_7 representing phases transformation – from trigonal (hR) to cubic (cF) crystal structure – during heating of the sample K_3HfF_7

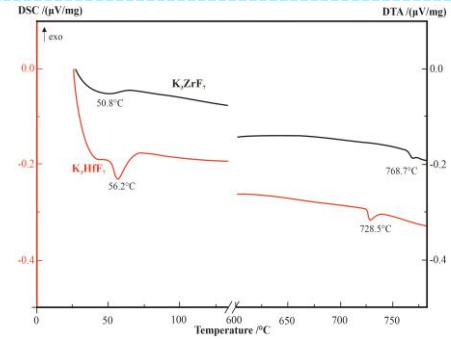

Figure 12. DSC/DTA record on K_3HfF_7 and K_3ZrF_7; heating curves

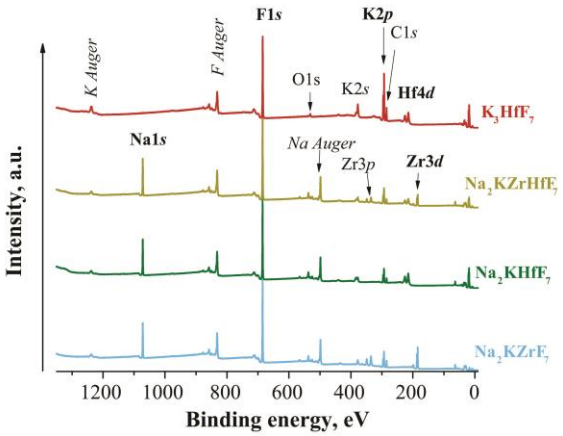

Figure 13. High resolution XPS survey spectra of the studied samples

References:

[1] L. Akselrud, Y. Grin. *J. Appl. Crystallogr.* 47 (2014) 803-805.
[2] V. Petříček, M. Dušek, L. Palatinus. *Z. Kristallogr.* 229 (2014) 345-352.
[3] K. Brandenburg, M. Berndt. *DIAMOND – Visual Crystal Structure Information System CRYSTAL IMPACT*, Postfach 1251, D-53002 Bonn.
[4] J. Mlynáriková, M. Boča et al. *J. Therm. Anal. Calorim.* 124 (2016) 973-987.
[5] P. Villars, K. Cenzual (Eds.), Pearson's Crystal Data. Crystal Structure Database for Inorganic Compounds, Release 2016/17, ASM International, Materials Park (OH), 2016.
[6] X. Lian, W.D. Yao et al. *Inorg. Chem.* 60 (2021) 19-23.
[7] M.V. Gorev, M.S. Molokeev et al. *J. Fluorine Chem. 241 (*2021) 109677.

Acknowledgements: This Project has been funded by the European Union's Horizon 2020 research and innovation programme on the basis of a grant agreement under the Marie Skłodowska-Curie funding scheme No. 945478; Slovak Research and Development Agency under the contract No. APVV-19-0270; Scientific Grant Agency of the Ministry of Education of the Slovak Republic and the Slovak Academy of Sciences under no. 2/0024/20.
O.M. is thankful to Dr. M. Poupon and E. Samolova (Institute of Physics of the Czech Academy of Science) for the X-ray single crystal diffraction analysis and Dr. M. Mičušík (Polymer Institute, Slovak Academy of Sciences) for the XPS measurements.